FULL PAPER

The "Electric Mondrian" as a Luminescent Solar Concentrator Demonstrator Case Study

Wilfried van Sark,* Panos Moraitis, Carlo Aalberts, Max Drent, Thom Grasso, Yves L'Ortije, Marc Visschers, Mattijs Westra, Rob Plas, and Wilko Planje

Inspired by the works of the Dutch artist Piet Mondrian, an Electric Mondrian has been developed built up from luminescent solar concentrator elements. It is based on differently colored square and rectangular elements of standard sizes based on multiples of 15 cm, as this is the standard size of the c-Si cells that are used at the sides of the elements. This paper describes the design requirements and choices that have been made in detail. The design is based on commercially available luminescent concentrator Perspex plates and solar cells. Performance testing showed that at a total size of 1 m² a light-to-electric power device efficiency is measured as 0.2%: the Electric Mondrian thus provides ∼2 W in full sun, and two mobile devices can be charged directly or via a built-in battery. The Electric Mondrian functions as a decorative energy-harvesting element indoors in the urban environment, and can be marketed as such.

1. Introduction

Today's photovoltaic (PV) solar energy market is dominated by flat plate silicon modules that are mounted on roofs in mostly optimal orientations and tilts, such that maximum power is reached around noon. However, this approach may be restrictive in the modern urban environment where tall buildings, small rooftops, and associated shading patterns coexist. Moreover, current PV technology hardly offers any form of flexibility for architects, designers, and engineers, since there is only one type of product of 1.6 m² standard size available in the market. In contrast, building-integrated PV (BIPV) modules and constructive elements are being developed that allow improved aesthetics, design, and functionality of PV elements.[1] One of these BIPV elements are Luminescent Solar Concentrators (LSCs), which can be cheap, transparent, and flexible and are able to operate under direct and

diffused light.[2–4] They are being developed to gradually replace windows and façades in modern buildings.[5]

The operating principle of LSCs is based on the absorption of incident photons by luminescent species (molecules or nanoparticles) that emit red-shifted photons, which are concentrated to the side of a waveguide by means of internal reflection. Solar cells that are mounted on these sides then collect photons and convert these into electricity. LSCs have been developed since the 1970s[2] as cost effective alternative to crystalline silicon PV technology. The present record efficiency of LSCs is 7.1%.[6] Only a few examples exist of >1 m² sized LSCs,[7,8] but they all suffer from low (∼1%) efficiencies, albeit that this is not considered important due to the aesthetical value of these applications. Ongoing research is directed toward surpassing the 10% efficiency barrier,[9] by addressing loss mechanisms in LSC operation such as self-absorption. New nanocrystal-based luminophores are under development that allow for larger sizes at high device efficiencies.[10–15] Most of LSC applications are in the phase of research, testing, or validation. At the moment, LSC devices are tested to replace sound barriers in Den Bosch, the Netherlands[16] or be used as roof tiles,[17] and, interestingly, as miniature chemical reactors.[18]

The main advantages of LSC technology for use as BIPV elements is the high level of flexibility in design, the ability to work under diffuse and direct irradiation[19] and potentially the low cost compared to conventional crystalline (BIPV) modules. However, the relatively low efficiency and the colored sheets that are currently used and affect human well being inside buildings[20] are the main challenges of the technology at the current state. In order to demonstrate the aesthetical quality of large size LSCs and to have users interacting and appreciating such a solar energy harvesting device an Electric Mondrian[1] based on LSCs is developed. The main concept of the project is to introduce LSCs to the public as a solar charger, a functionality that diminishes the aforementioned limitations. The power need for charging of mobile devices is relatively low (10–20 W) and can be met by the power output of the Electric Mondrian under regular lighting conditions. Portable size and colorful design make it suitable for decorative elements with the additional value of a functional device.

W. van Sark, P. Moraitis
Copernicus Institute of Sustainable Development, Utrecht University, Heidelberglaan 2, 3584 Utrecht, the Netherlands
E-mail: w.g.j.h.m.vansark@uu.nl
C. Aalberts, M. Drent, T. Grasso, Y. L'Ortije, M. Visschers, M. Westra, R. Plas, W. Planje
Centre for Technology and Innovation, University of Applied Sciences Utrecht, Oudenoord 700, 3513 EX Utrecht, the Netherlands

[1] Electric Mondrian™ has been registered as Trademark.

Inspired by the works of the Dutch artist Piet Mondriaan (1872–1944; he changed his name to Mondrian during his Paris period), in particular his colorful abstract works, such as the famous Broadway and unfinished Victory Boogie Woogie (**Figure 1**). It is constructed from several square and rectangular elements of different color and of standard sizes (length and width) of multiples of 15 cm, as this the standard size (156×156 mm^2) of the crystalline silicon cells that are used at the sides of the elements. The choice of a painting replica instead of a conventional stained glass window, such as reported by Kerrouche et al.,[21] was made to prove the flexibility of the device, and to help us study the effects of different colors on device efficiency. Instead of aiming directly for large-scale building applications, LSC devices can be promoted through the flexibility that can offer to designers. Devices that can power up mobile phones, tablets, laptops using solar energy could be easily created and offer a wide range of products to customers. As such, the present design may be considered a product integrated PV (PIPV) application[22] rather than a BIPV one. It can be used indoors behind windows as a decorative element that in addition can charge mobile devices. It invites users to interact and appreciate solar energy harvesting devices thereby appealing to their sustainability awareness.
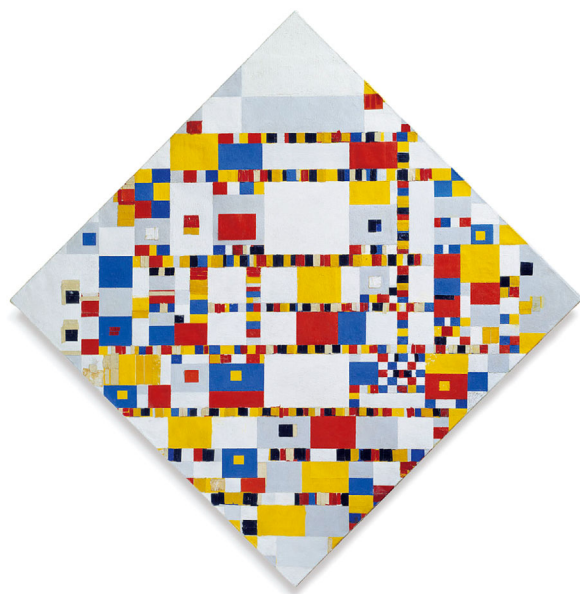
This paper describes in detail the design and development of the Electric Mondrian including performance testing.

2. Design and Development

2.1. Requirements

In designing the Electric Mondrian the following requirements were defined:

- Surface area of the prototype must be approximately 1 m^2.

Figure 1. Piet Mondrian, Victory Boogie Woogie (1942–1944), Gemeentemuseum The Hague, the Netherlands.

- Electrical output of the prototype must be at least several watts under full sun.
- Prototype has to be built using square and/or rectangular plastic plates of different color.
- Plate size (length, width) must be compatible with standard silicon solar cell size.
- A frame must hold plates and cells.
- Frame must allow hiding cabling and connectors to cells.
- Output of individual elements must be measurable separately.
- Prototype has to be portable.
- Electrical energy has to be stored, so that small devices (e.g., smartphones) can be charged, and
- Plates and solar cells must be commercially available.
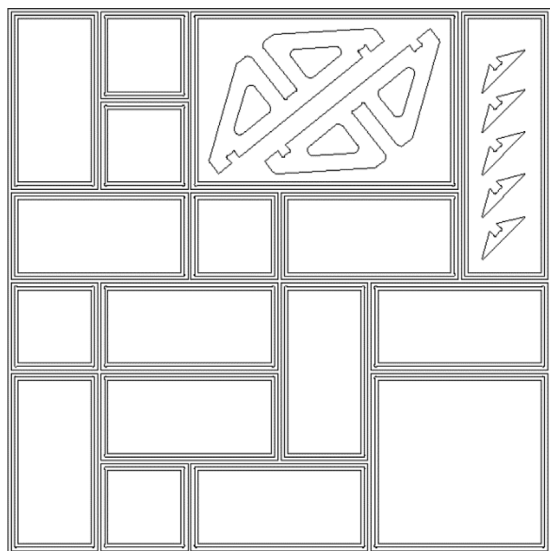
2.2. Design

2.2.1. Frame

Based on the availability of crystalline silicon solar cells (website Solarcapture Technologies) that could be cut to narrow slices of 0.5×15 cm^2 size,[23] the plastic plates should have dimensions of multiples of 15 cm. Luminescent acrylic plates (Perspex)[24] can be ordered to required sizes (Plasticsheets) in colors red, blue, green, orange, and yellow.

The frame was designed based on birch plywood as material. Two 1 m^2 sized panels of 18 mm (bottom) and 9 mm (top) thick could be processed by a CNC (computer numerical control) milling machine in order to obtain the necessary shape. The supports used to prevent the frame from falling over and to be able to test it in a realistic upright position, are milled out of the same 18 mm thick bottom plywood panel (see **Figure 2**). The prototype design uses 17 square and rectangle shaped holes in both panels, which house the acrylic sheets. The 5 mm thick acrylic sheets used in the prototype consist of a mixture of five different colors and five different shapes, as can be seen in **Table 1**. **Figure 3** shows a render of the prototype design.

The acrylic sheets rest on a 6 mm ridge inside the thickest panel (bottom), and 6 mm wide ducts for the cables are also located in this panel. These ducts run through all the beams in the frame and are just as deep as the ridges (9 mm). This leaves 2 mm of space on every side of the acrylic sheet. These gaps are filled up using 2 mm thick foam tape. This tape runs throughout the entire window, on every ridge, on both panels. In this way, the acrylic sheets are kept firmly in place and cannot move during, for example, transportation of the window, however the aperture area is somewhat smaller than listed in Table 1: all dimensions are 7 mm smaller, thus leading to an aperture area of 0.786 m^2. Both the ducts and the ridges can be seen in **Figure 4**. The ducts allow all solar cells to be connected to each other without external wiring. Only two wires exit the frame, a positive and a negative one.

2.2.2. Solar Cells

A total of 100 of solar cells are used in the prototype. They are cut from 156×156 mm^2 sized solar cells of 17.6% efficiency (open
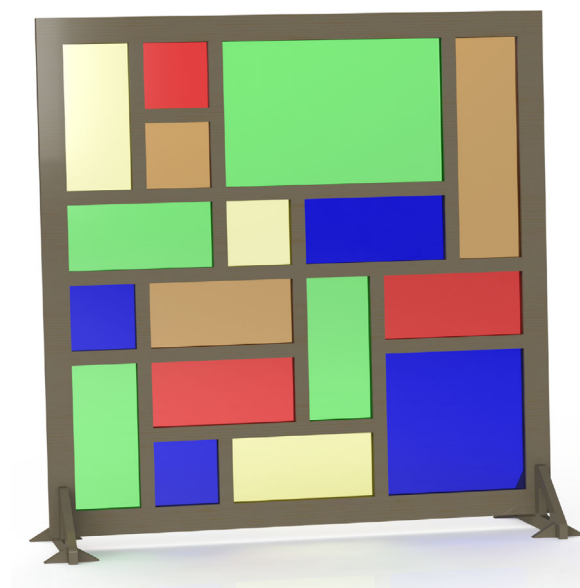
Figure 2. Milling design of plywood bottom plate of 1 m² size, including support parts. For the top plate the same milling design is used except for the support parts. The sizes of the squares and rectangles are shown in **Table 1**.

Figure 3. Render of the prototype design.

circuit voltage (V_{oc}) = 0.634 V, short circuit current (I_{sc}) = 35.0 mA/cm², fill factor (FF) = 0.79)[24] down to a size of 5×145 mm², which would lead to an I_{sc} of 254 mA per cell under standard test conditions (1,000 W/m² solar intensity at AirMass 1.5 spectrum and 25°C cell temperature). Soldered silver tabs to the cells are used for interconnection. For the smallest sheet four solar cells are used, so the total voltage will be ~2 V at maximum power, as they are connected in series and voltage at maximum power is ~0.5 V per cell. For the total frame, the 100 cells will generate ~50 V. Current will be ~25–50 mA, and estimated power about 10–20 W at sunny conditions.

The solar cells need to be attached to the acrylic sheets, which can be done by means of a transparent adhesive. To minimize optical losses, the adhesive should have a refractive index similar to that of acrylic sheets (1.45).

For every acrylic sheet with solar cells, a hole of 6 mm diameter serves as an access point to the cable duct from the outside and contains two female pin headers (17 holes in total, 34 female pin headers). These headers have been soldered to the solar cells and cables, allowing every set of solar cells that are glued to an acrylic sheet, to be measured individually.

Male headers are to be put in the female headers whenever a set of multiple acrylic sheets needs to be measured, or whenever the window is put in use and all cells must be connected in series. The

Table 1. Colour and size specifications of sheets, with 5 mm thickness.

Color	Absorption maximum (nm)	Emission maximum (nm)	Size (mm²)	Amount	#Solar cells
Blue	410	430	315 × 315	1	8
			315 × 145	1	6
			145 × 145	2	4
Green	480	500	485 × 315	1	10
			315 × 145	3	6
Yellow	530	550	145 × 145	1	4
			315 × 145	2	6
Orange	560	580	485 × 145	1	8
			315 × 145	1	6
			145 × 145	1	4
Red	580	610	315 × 145	2	6
			145 × 145	1	4

Total amount of solar cells is 100. Total sheet area is 0.84 m².

Figure 4. Cable ducts and ridges design detail.

connection scheme is shown in **Figure 5**. Thus, it is possible to realize different connection schemes for the PV-panels.
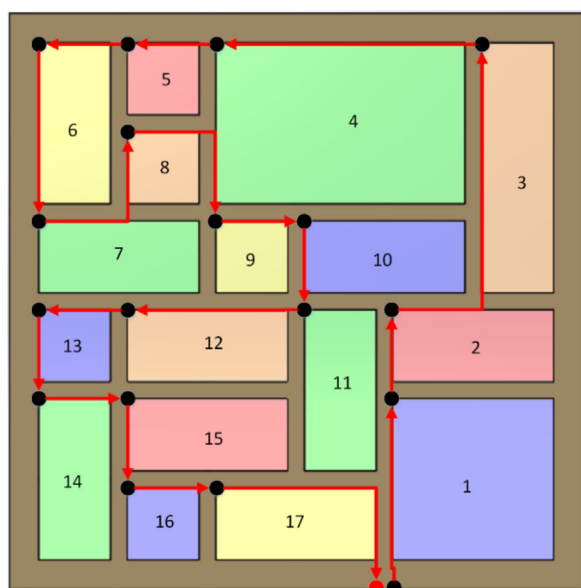
It will be clear that due to the different size and color of the elements the currents (e.g., short circuit current) will differ between elements. Connecting all cells in series will increase the voltage, but the element with the lowest current will determine the final current for the whole device. Clearly, this will lead to non-optimal connection regarding maximum power. Optimization of colors (choice of luminophores) and sheet dimensions to reach high efficiencies will be done in future work, using Monte-Carlo based ray-trace modeling.[25]
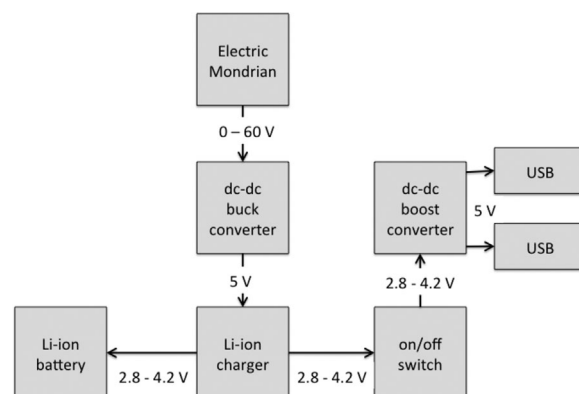
2.2.3. Electronics

In order to minimize the effect of potential shading, a bypass diode will be connected in parallel to the cells that are attached to one acrylic sheet.

The Electric Mondrian would supply about 50 V, which is to be converted down to a voltage that can charge a lithium-ion (Li-ion) battery to store electricity generated during the day. A dc–dc (buck) converter will be used for this conversion.[26] After the voltage is reduced to the required amount, it can be used to charge the batteries. To prevent the batteries from getting damaged due to over- and under voltage a Li-ion charger will used. The output voltage of the Li-ion battery will be ranging from 2.8 to 4.2 V. To charge a phone or power another USB device, 5 V is needed, so a dc-dc (boost) converter will be used.

The physical output consists of two USB-ports, that both will supply the USB 2.0 standard of 500 mA. This is enough to power most USB devices and charge mobile phones. The maximum battery load is 3,000 mA, if the load is higher the Li-ion protection will disconnect the battery. **Figure 6** shows an overview of the electronics schematics.

Figure 6. Electronics functional schematics.

All electronics components need to be fitted in a box, which is preferably part of the prototype construction. The design of this box is shown in **Figure 7**, fitted in the support of the prototype, and a computer render with transparent walls for the box, allowing the parts inside to be seen. The red and black 4 mm banana plugs are inputs to which the plus and minus cable from the frame is connected.
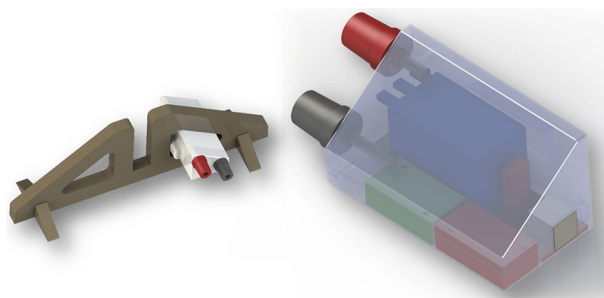
3. Results and Discussion

3.1. Construction

3.1.1. Frame and Solar Cells

The first part of the prototype made was the frame and the supports. This was milled on a CNC milling machine. The entire milling process took roughly 2 h. Acrylic sheets and solar cells have been ordered from Plastic Sheet[26] and Solar Capture Technologies[27]. The cells included soldered tabbing, as can be seen in **Figure 8**, which meant a reduction in aperture area of about 30%, due to the 1.5 mm wide tabbing.

The first step in the assembly of the prototype was attaching the solar cells to the acrylic sheets. A thermosetting polyurethane (MY-145, from Mypolymers[28]), with refractive index of 1.45) was used as transparent adhesive glue. The entire gluing and curing process and soldering of the cells took 3 days. Some examples

Figure 5. Connection scheme of the 17 elements.

Figure 7. Casing design ($11 \times 6 \times 6 \, cm^3$) fitted in support ($32 \times 13 \times 11 \, cm^3$), with transparent sides for better view. In reality, the casing is white.

ADVANCED
SCIENCE NEWS
www.advancedsciencenews.com

Solar RRL
www.solar-rrl.com

FULL PAPER

can be seen in **Figure 9**. Subsequently, all these finished acrylic sheets were placed inside the bottom panel, on top of a layer of foam tape. This foam tape prevents the acrylic sheet from getting scratched and from being moving around in the frame. Cutting the foam tape to size and applying this to both sides of the frame took about 45 min.

Once all sheets with the attached solar cells were in place, they could be connected up to each other. All solar cells are connected in series; this is to avoid a complex electrical circuit to convert different currents to one usable current. In this configuration all the voltages are added to yield a higher voltage with a lower current, at the expense of lower overall power output. The solar cells are connected using $0.75\,mm^2$ cables. The cables used for the connections run throughout the entire frame, in the cable ducts, and cannot be seen from the outside. Parallel to every set of PV-panels that is part of one acrylic sheet, a bypass diode has been placed. These have been soldered onto the tabbing wires, as can be seen in **Figure 10**.

In the frame, there are 17 holes, one per acrylic sheet. These holes contain the female pin headers that have been secured in place using hot glue. One side of the header is the positive side of sheet 1 and the other side is the negative side of sheet 2. If these two sides are connected, for instance by using a jumper, the sheets will be connected in series. In this configuration it is possible to exclude solar cells from being measured in case they are broken or faulty, by skipping the headers that belong to that sheet. For instance, if it is necessary to bypass sheet 4, the jumpers used to connect panels 3, 4, and 5 must be removed (see also Figure 5). A wire from header 3 must be placed to connect to header 5, the wire must connect the positive side of header 3 to the negative side of header 5. In this situation, the total output excluding sheet #4 can be measured.

3.1.2. Electronics

The current from the Electric Mondrian enters through the 4 mm banana plugs in the electronic components casing. The input is protected to prevent reverse polarity. The high voltage input, between 0 and 60 V, is converted down to 5 V so the lithium charger can charge the Li-ion cells. Three 3.7 V 2,050 mAh Li-ion cells are included. These lithium cells are connected in parallel and act as one Li-ion cell at a total of 3.7 V and 6,150 mAh. The charger also has a protection against over discharging, which starts at 2.8 V and an overcurrent protection of 3 A. All components and the finished casing can be seen in **Figure 11**. The casing, which houses all the electrical components, was 3D printed using one of the 3D printers available in house, which took about 3.5 h.

The USB ports can be toggled on and off, by a switch (Figure 11, top left). If no devices require charging, it should be toggled off. The output from the USB charger is two times 5 V at 0.5 A. It is possible to provide quick charge for mobile devices, to enable this

for Android a 100-Ω resistor must be placed between the data pins of one of the USB ports. To enable this for Apple devices a more complicated resistor network is required. The current is limited to two times 0.5 A, because of the current protection in the charge module of 3 A. The maximum power of the current limiter at low voltage is $3\,V \times 3\,A = 9\,W$. The power that the step-up converter draws is $5V \times 1A/0.8 = 6.25\,W$ at 80% efficiency.
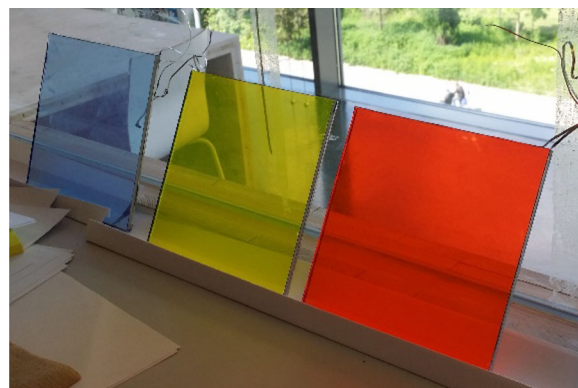
3.1.3. Final Prototype

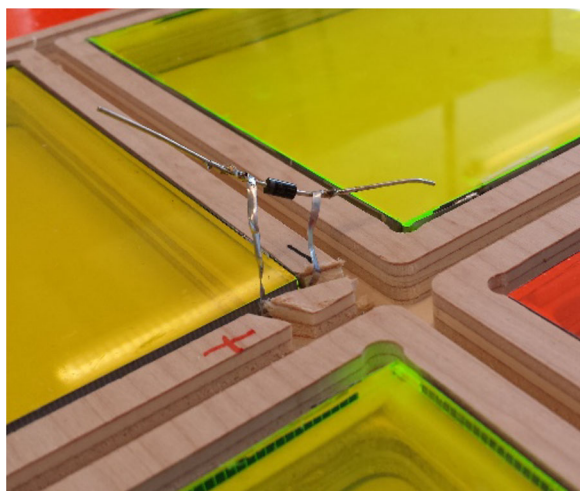A photograph of the final prototype is shown in **Figure 12**.

3.2. Performance Testing

An outdoor test of the complete device as well as of individual sheets was performed on a sunny day (June 11, 2015) in Utrecht, the Netherlands, at noon. The in-plane irradiance was measured to be $600\,W/m^2$, while the device was standing upright (as in Figure 12), and was constant during the measurements. Ambient temperature was 20 °C, with a light breeze and relative humidity of 50%. A V_{oc} of 59.8 V and I_{sc} of 20.7 mA were measured for the prototype. Assuming $FF = 0.75$ of the c-Si solar cells used, maximum power was 0.928 W. Using an aperture area of $0.786\,m^2$, the light-to-electric power efficiency is 0.197%. With the full area of the prototype ($1\,m^2$), efficiency is 0.155%. We have tested the prototype indoors behind window to find that on a sunny day (June 12, 2015) the battery is nearly fully charged after about 12 h, thus providing about 20 Wh of energy for charging several mobile devices.

The results for the individual sheets are shown in **Figure 13**. It is clear that the larger the sheet the lower the efficiency. The smallest red sheet (with four cells) has the largest efficiency of 2.1%, while the lowest efficiencies are determined for the blue sheets, as a result of high transmission and low absorption (see also Figure 12). If the electrical circuitry would be optimized, that is, maximum power of all sheets could be added, a device efficiency of 0.95% (aperture area) could be reached, generating 7.5 W. In fact, disconnecting the blue sheets from the circuit would improve the efficiency to this level. At this power level, an

Figure 8. Solar cell ($5 \times 145\,mm^2$), with 1.5 mm wide soldering tabbing.

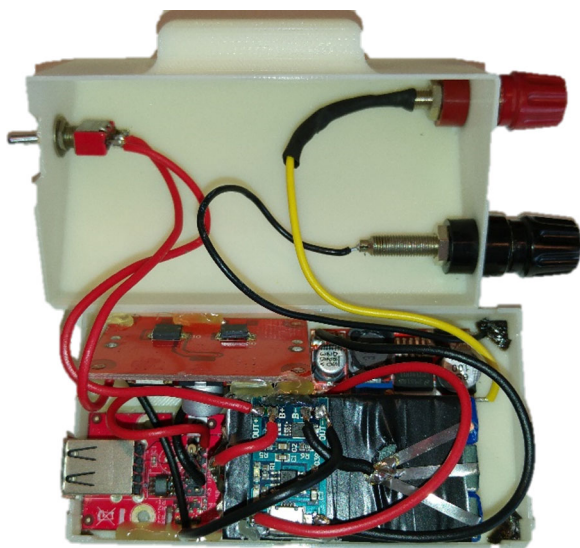**Figure 9.** A batch of finished $145 \times 145\,mm^2$ sheets, with solar cells attached.

Figure 10. Bypass diode connected to sheet in the frame.

iPhone SE (with 6.21 Wh battery capacity[29]) could be charged in about 1 h at full sun conditions. This would make the Electric Mondrian attractive for users, also to encourage them to interact with the device, and thus appreciate the usefulness of colorful sustainable energy harvesting options.

4. Conclusion and Outlook

This paper described the design and fabrication of an Electric Mondrian, inspired by the colorful works of the Dutch artist Piet Mondrian. We have employed acrylic sheets that function as luminescent solar concentrators and attached standard c-Si solar cells to each side. Solar energy harvested is either stored in an on-board Li-ion battery, or directly used for charging mobile devices.
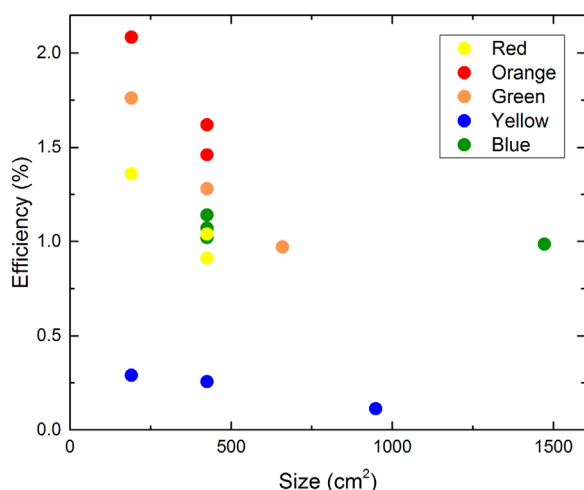

Figure 12. Photograph of final prototype, indoors.

At a total area of nearly 1 m^2 under full sun conditions the Electric Mondrian delivers 1 W of power in the present electric configuration, which could be 7.5 W after optimized reconfiguration.

Since its conception the Electric Mondrian has received quite some attention in the national newspapers and many requests have been received for purchase. The Electric Mondrian as a device (product) is considered a niche application (solar charging), which can cover a rather new need that emerged over the last few years in a sustainable way. However, the present cost of the prototype is too high for market success. Presently, stained leaded-glass of a design such as in Figure 3 would cost 300–500 €/m^2. The fact that an Electric Mondrian has a stained leaded-glass look with an additional benefit of charging two mobile devices simultaneously makes it attractive, and a little higher cost compared to stained leaded-glass may very well be marketable. As such, the Electric Mondrian rather can be classified as a product integrated PV (PIPV) application, and can be marketed as such.

In future work, our main priority is to further develop LSC technology, as it is the one that offers a high level of flexibility

Figure 11. Electronic components in the 3D printed box.

Figure 13. Efficiency of individual acrylic sheets as a function of sheet area.

(geometry, color) and focus on how to improve efficiency and reduce the cost. Some of the parameters that are going to be thoroughly studied in the simulations are the use of a different selection of luminophores, the possibility to use back reflectors in some of the sheets and the effect of refractive coatings. Combined with a new design for the wiring and the dc–dc conversion we believe that we can significantly increase the device performance.

Acknowledgments

[1] Cerón, I., Caamaño-Martín, E., Neila, F.J., "State-of-the-art" of building integrated photovoltaic products, *Renew. Energy* **2013**, *58*, 127.

[2] Goetzberger, A., Greubel, W., Solar energy conversion with fluorescent collectors, *Appl. Phys.* **1977**, *14*, 123.

[3] Van Sark, W.G.J.H.M., Barnham, K.W.J., Slooff, L.H., Chatten, A.J., Büchtemann, A., Meyer, A., McCormack, S.J., Koole, R., Farrell, D.J., Bende, E-E., Burgers, A.R., Budel, T., Quilitz, J., Kennedy, M., Meyer, T., De Mello Donegá, C., Meijerink, A., Luminescent Solar Concentrators– A review of recent results, *Opt. Express* **2008**, *16*, 21773.

[4] Van Sark, W.G.J.H.M., Hellenbrand, G.F.M.G., Bende, E.E., Burgers, A.R., Slooff, L.H. Annual Performance of the Fluorescent Solar Concentrator, Proc. 23rd European Photovoltaic Solar Energy Conference **2008**, 198.

[5] Debije, M.G., Verbunt, P.P.C., Thirty years of luminescent solar concentrator research: Solar energy for the built environment, *Adv. Energy Mater.* **2012**, *2*, 12.

[6] Slooff, L.H., Bende, E.E., Burgers, A.R., Budel, T., Pravettoni, M., Kenny, R.P., Dunlop, E.D., Büchtemann, A., A luminescent solar concentrator with 7.1% conversion efficiency, *Phys. Status Solidi RRL* **2008**, *2*, 257.

[7] Aste, N., Tagliabue, L.C., Del Pero, C., Testa, D., Fusco, R, Performance analysis of a large-area luminescent solar concentrator module, *Renew. Energy* **2015**, *76*, 330.

[8] Viswanathan, B., Reinders, A., De Boer, D.K.G., Ras, A., Zahn, H., Desmet, L., System engineering and design of LSC-PV for outdoor lighting applications. Proc. 27th European Photovoltaic Solar Energy 28 Conference and Exhibition **2012**, 4273.

[9] Van Sark W.G.J.H.M, Recent developments in luminescent solar concentrators. Proc. SPIE 2014, Next Generation Technologies for Solar Energy Conversion V 9178, 917804. 2014 to 9178 2014, 917804. **2014**.

[10] Krumer, Z., Pera, S.J., Van Dijk-Moes, R.J.A., Zhao, Y., De Brouwer, A.F.P., Groeneveld, E., Van Sark, W.G.J.H.M., Schropp, R.E.I., De Mello-Donegá, C., Tackling self-absorption in Luminescent Solar Concentrators with type-II colloidal quantum dots, *Sol. Energ. Mat. Sol. Cells* **2013**, *111*, 57.

[11] Erickson, C.S., Bradshaw, L.R., McDowall, S., Gilbertson, J.D., Gamelin, D.R., Patrick, D.L., Zero-Reabsorption Doped-Nanocrystal Luminescent Solar Concentrators, *ACS Nano* **2014**, *8*, 3461.

[12] Meinardi, F., Colombo, A., Velizhanin, K.A., Simonutti, M., Lorenzon, M., Beverina, L., Klimov, V.I., Brovelli, S., Large-area luminescent solar concentrators based on 'Stokes-shift-engineered' nanocrystals in a mass-polymerized PMMA matrix, *Nat. Photonics* **2014**, *8*, 392.

[13] Meinardi, F., McDaniel, H., Carulli, F., Colombo, A., Velizhanin, K.A., Makarov, N.S., Simonutti, R., Klimov, V.I., S. Brovelli, S., Highly efficient large-area colourless luminescent solar concentrators using heavy-metal-free colloidal quantum dots, *Nat. Nanotechnol.* **2015**, *10*, 878.

[14] Mirershadi, S., Ahmadi-Kandjani, S., Efficient thin luminescent solar concentrator based on organometal halide perovskite, *Dyes Pigm.* **2015**, *120*, 15.

[15] Ten Kate, O.M., Krämer, K.W., Van der Kolk, E., Efficient luminescent solar concentrators based on self-absorption free Tm^{2+} doped halides, *Sol. Energ. Mat. Sol. Cells* **2015**, *140*, 115.

[16] Kanellis, M., De Jong, M.M., Slooff, L., Debije, M.G., The solar noise barrier project: 1. Effect of incident light orientation on the performance of large-scale luminescent solar concentrator noise barier, *Renew. Energy* **2017**, *103*, 647.

[17] Reinders, A.H.M.E., Doudart de la Grée, G., Papadopoulos, A., Rosemann, A., Debije, M.G., Cox, M., Krumer, Z., Leaf roof — Designing luminescent solar concentrating PV roof tiles, Proc. 43rd IEEE Photovoltaic Specialists Conference **2016**, 3447.

[18] Cambié, D., Zhao, F., Hessel, V., Debije, M.G., Noël, T., A Leaf-Inspired Luminescent Solar Concentrator for Energy-Efficient Continuous-Flow Photochemistry, *Angew. Chem. Int Ed* **2017**, *56*, 1050.

[19] Debije, M.G., Rajkuma, V.A., Direct versus indirect illumination of a prototype luminescent solar concentrator, *Solar Energy* **2015**, *122*, 334.

[20] Vossen, F.M., Aarts, M.P.J., Debije, M.G., Visual performance of red luminescent solar concentrating windows in an office environment. *Energ. Buildings* **2016**, *113*, 123.

[21] A. Kerrouche, D.A. Hardy, D. Ross, B.S. Richards, Luminescent solar concentrators: From experimental validation of 3D ray-tracing simulations to coloured stained-glass windows for BIPV *Sol. Energ. Mat. Sol. Cells* **2014**, *122*, 99.

FULL PAPER

[22] G. Apostolou, A.H.M.E. Reinders, Overview of design issues in product-integrated Photovoltaics *Energy Technol.* **2014**, *2*, 229.

[23] Baistow, I., Dunnill, S., Morrison, D.J., Advanced Manufacturing techniques for silicon concentrator modules. Proc. 28th European Photovoltaic Solar Energy Conference, **2013**; 587.

[24] Plastic Sheets, **2016**. www.plasticsheets.com (accessed 18 November 2016).

[25] R.W. Erickson, D. D. Maksimovic, *Fundamentals of Power Electronics* Springer, New York, **2001**.

[26] Farrell D.J., **2016**; pvtrace: optical ray tracing for photovoltaic devices and luminescent materials. doi.org/10.5281/zenodo.12820 (accessed 18 November 2016).

[27] Solar Capture Technologies, **2016**. www.solarcapturetechnologies.com (accessed 18 November 2016).

[28] Mypolymers, **2016**. www.mypolymers.com (accessed 18 November 2016).

[29] GSMarena, **2016**. www.gsmarena.com/apple_iphone_se-7969.php (accessed 18 November 2016).